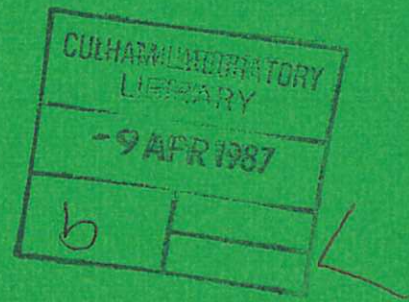




UKAEA

Preprint



INFLUENCE OF DISCHARGE DYNAMICS ON IMPURITY CONFINEMENT IN HIGH DENSITY OHMICALLY HEATED TOKAMAK PLASMAS

R. BARNESLEY
S. J. FIELDING
N. C. HAWKES
J. HUGILL
P. C. JOHNSON
W. MILLAR
N. J. PEACOCK
K. B. AXON
K. D. EVANS

CULHAM LABORATORY
Abingdon, Oxfordshire

1987

This document is intended for publication in a journal or at a conference and is made available on the understanding that extracts or references will not be published prior to publication of the original, without the consent of the authors.

Enquiries about copyright and reproduction should be addressed to the Librarian, UKAEA, Culham Laboratory, Abingdon, Oxon. OX14 3DB, England.

INFLUENCE OF DISCHARGE DYNAMICS ON
IMPURITY CONFINEMENT IN HIGH DENSITY
OHMICALLY HEATED TOKAMAK PLASMAS

R. Barnsley*, S.J. Fielding, N.C. Hawkes, J. Hugill, P.C. Johnson,
W. Millar, N.J. Peacock, K.B. Axon and K.D. Evans*

Culham Laboratory, Abingdon, Oxon. OX14 3DB, U.K.
(Euratom/UKAEA Fusion Association)

*Department of Physics, University of Leicester, Leicester, U.K.

ABSTRACT

A correlation has been found between impurity confinement time and discharge dynamics in ohmically heated tokamak discharges. Experiments on DITE using injected impurities show that, at high plasma densities, long confinement times are obtained in constant density discharges, short confinement times for rising density. These observations are discussed and compared with impurity behaviour in other tokamaks.

(Submitted for publication in Physical Review Letters)

PACS Number 52.25.Vy, 52.55.Fa

October 1986

The extra radiation and dilution of the background fuel due to the presence of impurities in projected tokamak fusion reactors are matters of continuing concern. Neoclassical theory¹ generally predicts an accumulation of impurities in the centre of the discharge unless the temperature gradient screening effect is sufficiently strong. However, the results from existing experiments, recently reviewed by Isler², are confusing. Long impurity confinement times and/or impurity accumulation have been observed in some cases: for example, in deuterium discharges in ISX-B³, in the absence of the sawtooth instability in Pulsator⁴ and DIII⁵, in H-mode discharges on ASDEX⁶ and after refuelling by pellets⁷, and in low current high density discharges in T-10⁸. More generally, however, the impurity confinement time, τ_{imp} , is of the same order as that of the main plasma ions and impurity accumulation is not observed. In this latter context, measurements of τ_{imp} on Alcator over a wide range of conditions were well represented by a formula involving the main discharge parameters⁹, which appears to fit the data from several other devices².

In this paper we report new results from experiments in ohmically heated, helium discharges in DITE tokamak. At high density the central confinement time of injected impurities can be varied by at least a factor of five without changing the main discharge parameters. The effect is produced by altering the rate of gas puffing and it correlates with the time rate of change of line average electron density, $d\bar{n}_e/dt$. Large values of τ_{imp} and impurity accumulation of intrinsic impurities are observed when the discharge is refuelled by recycling only and $d\bar{n}_e/dt$ is approximately zero. Smaller values of τ_{imp} and a dependence on \bar{n}_e like that observed on Alcator are obtained when \bar{n}_e is rising.

The majority of data were obtained with 100kA plasma current, 2.6T toroidal field, and graphite limiter radius of 0.21m. Non-recycling metallic impurities, Al, Si or Ti were injected into the torus by laser ablation from thin films¹⁰, thus providing a reproducible source of energetic (1-3eV) neutral impurity atoms. In all cases the injected impurity acted as a small perturbation on the plasma electron content, and no associated increase in electron density could be detected by microwave interferometry. Only in the case of titanium injection was there any evidence of a substantial increase in total plasma radiation. Most data were obtained with aluminium. Z_{eff} was estimated to be ~ 3 , at the time of injection, in the medium and high density discharges.

Line radiation from the injected impurities was measured by visible, normal incidence, grazing incidence and X-ray spectroscopy. The normal and grazing incidence spectrometers had fixed horizontal lines of sight through the plasma centre. The X-ray instrument was a Bragg flat crystal spectrometer¹¹, with six separate crystals on a rotating mount. In survey mode, with the crystal mount rotating at up to 5Hz, this gave repeated scans of the spectral band determined by the crystal selection, typically 2Å-24Å in these experiments. The scan time of any one feature was 100 microseconds. In monochromator mode, with the crystal fixed at a specified diffraction angle, chord-average measurements of emission from particular lines were made with sub-millisecond time resolution. By tilting the whole instrument with respect to the horizontal plane, it was also possible to build up spatial profiles, with 20mm resolution, on a shot by shot basis. Spatially resolved broadband X-ray emission measurements were made by two Si(Li) detector camera systems, one viewing vertically, the other horizontally, with a spatial resolution of 10mm. High pass filters were

used, with 1keV low energy cut off. Other plasma parameters were measured by conventional diagnostic techniques.

It became obvious during experiments with varying gas feed that there was a correlation between impurity confinement and the time variation of plasma density. Fig.1 shows the time histories of line and broadband emission for aluminium injection into two discharges of similar plasma density, $\bar{n}_e \sim 6 \times 10^{19} \text{m}^{-3}$, but differing values of $d\bar{n}_e/dt$. For the first 20ms after impurity injection the plasma density is rising in both cases and the two discharges exhibit similar behaviour. For times greater than this, when the discharge dynamics differ, the signals are quite dissimilar. The central electron temperatures in the two cases, measured by Thomson scattering, remain approximately constant during the time shown (see also Fig.4c). Measurements of the ratio β_p/\bar{n}_e , derived from the diamagnetic loop and microwave interferometer diagnostics, and the ratio of A λ XIII and A λ XII line emissions also agree with a near constant temperature. Hence we interpret changes in the line emissions, after correcting for the different electron density variation as changes in the impurity concentrations. We define an impurity confinement time, τ_{imp} , as the 1/e decay time of the ratio of line emission/ \bar{n}_e . It is clear from Fig.1 that impurities injected into discharges with approximately constant density have much longer confinement times than those injected into discharges with rising density. An alternative explanation invoking changes in recycling behaviour of the injected impurity is considered to be improbable, since there is no experimental evidence to date that Al or Si recycle, and the contrast in their behaviour with that of neon or argon, strongly recycling elements, is striking. Intrinsic impurities also show a difference in confinement between the two types of discharge. In Figs.1a and 1b, the aluminium line

emission shows a slow decrease for the long confinement case, whereas the broadband emission, Fig.1c, shows a slow continuing increase after the initial fast rise, indicating a slow increase in intrinsic impurity density. In contrast, for the short confinement case, there is evidence of a slow decrease in intrinsic impurity density, since the broadband emission returns to its original level after the decay of the aluminium line emission whereas the electron density has increased by some 25%.

Spatial scans of AlXIII and AlXII line emission were built up shot by shot from a series of similar discharges. These are shown in Fig.2 as a function of chord height. Chord average emission measurements through the plasma axis, using these lines, therefore provide information about impurity behaviour in this central core. Little difference can be seen between the profile shapes in the central region for long and short confinement cases. In this region the profiles are dominated by the radial variation of the excitation rates rather than the spatial form of the impurity concentration. In the outer regions there is a noticeable difference between the two cases. This is discussed below where examples of the time evolution of profiles are shown. Emission lines of less highly ionised ions of aluminium, e.g. AlXI, AlX, were also recorded but it was difficult to derive useful information from the data because of the low signal to background ratio many tens of milliseconds after injection. Only the core ions were used for detailed analysis.

Figure 3 shows results obtained from aluminium injection into two series of discharges, one at 100kA, the other at 150kA, for $\frac{d\bar{n}_e}{dt} \sim 0$ (referred to as 'constant density') and for $\frac{d\bar{n}_e}{dt} > 9 \times 10^{19} \text{m}^{-3} \text{s}^{-1}$ ('rising density'), for a range of values of electron density at the time of impurity injection. At low density there is no difference, within

experimental errors, between the impurity confinement in constant and rising density discharges. For constant density the confinement time increases with density up to the highest electron density achieved. In contrast, discharges with rising density show a clear maximum confinement time and then a decrease with density. The density at which this maximum occurs is higher at 150kA than at 100kA. The results shown in Fig.3 suggest a bifurcation in impurity confinement but high density discharges with intermediate values of \overline{dn}_e/dt have not yet been studied and hence clarification of this point awaits further experimental work.

Control of \overline{dn}_e/dt in these experiments was effected by changing the gas feed rate. However there was a delay of up to several tens of milliseconds between switching on or off the gas valves and a change in the value of \overline{dn}_e/dt . It was observed that the change in impurity confinement took place when \overline{dn}_e/dt altered rather than at the time when the gas feed rate was changed. This can be seen in Fig.4, which shows the behaviour of λ XIII and X-ray emission for λ injection into a discharge where the electron density was initially constant and the confinement time long. At 400ms the gas feed is again turned on but the electron density is not observed to change significantly until 440ms; only at this time is there a change in the behaviour of the X-ray signals and a switch to the short confinement mode. In the spatially resolved spectroscopic data of Fig.4a, the λ XII signals have been normalised at their peak values; for the X-ray continuum, Fig.4b, normalisation is at a time just prior to the λ injection. In this way changes in the outer, less efficiently radiating, regions of the plasma are more easily seen. Both sets of signals show similar features. During the initial long confinement phase there is a

slow evolution and narrowing of the impurity profile. At $\sim 440\text{ms}$ $d\bar{n}_e/dt$ is increased and there is a quite rapid ($\sim 40\text{ms}$) rearrangement of the profile to a broader shape, shown clearly by the increase in signal in the outer channels, and then the decay of all channels with the short confinement time constant. Separate X-ray data on the intrinsic impurities show that there is a gradual accumulation of impurities on axis during the long confinement phase, and a decrease in impurity density over the whole core during the short confinement phase. The mhd activity, detected by Mirnov coils, remains at a low level over the whole discharge period. It is also found that there is no significant difference in energy confinement between long or short impurity confinement discharges, at similar density.

The results from DITE show some similarity with those reported on PULSATOR⁴, where accumulation of intrinsic impurities was observed during a density plateau in high density discharges. An additional gas puff was observed to suppress the accumulation and, by the use of krypton rather than hydrogen, it was shown that the reduction of axial impurity density was due to a change in transport rather than a reduced source term. On DIII tokamak⁵ a bifurcation in impurity behaviour was observed in the first 100ms of ohmic heated discharges; so called type 'S' discharges exhibited sawteeth and no impurity accumulation, whereas type 'O' were characterised by lack of sawteeth and impurity confinement times of several hundred milliseconds leading to increasing impurity density and eventual disruption. On DITE no obvious difference in sawtooth characteristics is observed between long and short confinement cases. The X-ray signals in Fig.1c show sawteeth throughout, with period linearly proportional to density and approximately constant amplitude. Recent observations on T-10 also showed short ('S') and long ('B') impurity confinement times for injected

impurities⁸. However in these experiments differences in energy and background plasma transport were also inferred, in contrast with the results from DITE. The extensive study of the confinement of injected impurities in Alcator^{9,12} has resulted in the derivation of a confinement time scaling law, valid when mhd activity is weak. This scaling law has no explicit density dependence and hence no meaningful comparison can be made with DITE long confinement discharges, where τ_{imp} can vary by an order of magnitude, depending on density. In fact, on Alcator the variation of τ_{imp} with density shows a similar form to the DITE short confinement data of Fig.3. The neoclassical-type confinement times, observed in several tokamaks (see earlier references), do not fit the Alcator law. The results from the DITE experiments suggest that the differences in confinement observed between the various machines may well result from differences in discharge dynamics. However, the published data is not sufficiently complete to confirm this. It is possible that changes in $d\bar{n}_e/dt$ lead to or are evidence of internal rearrangement of the density profile, causing a change in impurity transport. More direct evidence of this is seen on ASDEX where pellet refuelling leads to a distinctly different density profile to that from gas refuelling, and a marked difference in impurity confinement is noted in the two cases⁷.

In summary, in ohmically heated discharges on DITE we have observed a controlled and reproducible dependence of impurity confinement on discharge dynamics. Long confinement is observed at constant plasma density at all values of density up to the highest attainable, $\bar{n}_e = 9 \times 10^{19} \text{ m}^{-3}$. A narrowing of the profiles of both injected and intrinsic impurities is observed with the latter showing a gradual axial accumulation. The

impurity profile is found to be constantly evolving. For rising density and densities above a current dependent lower limit a considerably shorter impurity confinement is measured. A less peaked impurity profile is observed, which remains constant in shape during its decay.

We are grateful to the other members of the DITE physics team for help in obtaining the experimental data, and to the operations team for maintaining and operating the tokamak.

REFERENCES

1. S.P. Hirshman, D.J. Sigmar, Nucl. Fusion 21 (1981) 1079.
2. R.C. Isler, Nucl. Fusion 24 (1984) 1599.
3. K.H. Burrell, et al., Nucl. Fusion 21 (1981) 1009.
4. W. Engelhardt, et al., in Plasma Physics and Controlled Nuclear Fusion Research (Proc. 7th Int. Conf., Innsbruck, 1978), Vol.1, IAEA, Vienna (1979) 123.
5. G.L.Jahns, et al., Nucl. Fusion 22 (1982) 1049.
6. M. Keilhacker, et al., in Plasma Physics and Controlled Nuclear Fusion Research (Proc. 10th Int. Conf., London, 1984), Vol.1, IAEA, Vienna (1985) 71.
7. H. Niedermeyer, et al., in Controlled Fusion and Plasma Heating (Proc. 13th Europ. Conf., Schliersee, 1986) Vol.10c, EPS, Schliersee, Pt.1, (1986) 168.
8. A.A. Bagdasarov, et al., in Controlled Fusion and Plasma Physics (Proc. 12th Europ. Conf., Budapest, 1985) Vol.9F, EPS, Budapest, Pt.1, (1985) 207.
9. E.A. Marmor, J.E. Rice, S.L. Allen, Phys. Rev. Lett. 51 (1983) 455.
10. E.A. Marmor, Rev. Sci. Instrum. 46 (1975) 1149.

11. R. Barnsley, K.D. Evans, N.J. Peacock, N.C. Hawkes, Proc. 6th Topical Conf. on High Temperature Plasma Diagnostics, Hilton Head Island, South Carolina, USA. Rev. Sc. Instrum. 57 (1986) 2159.
12. E.A. Marmor, J.E. Rice, J.L. Terry, F.H. Sequin, Nucl. Fusion 22 (1982) 1567.

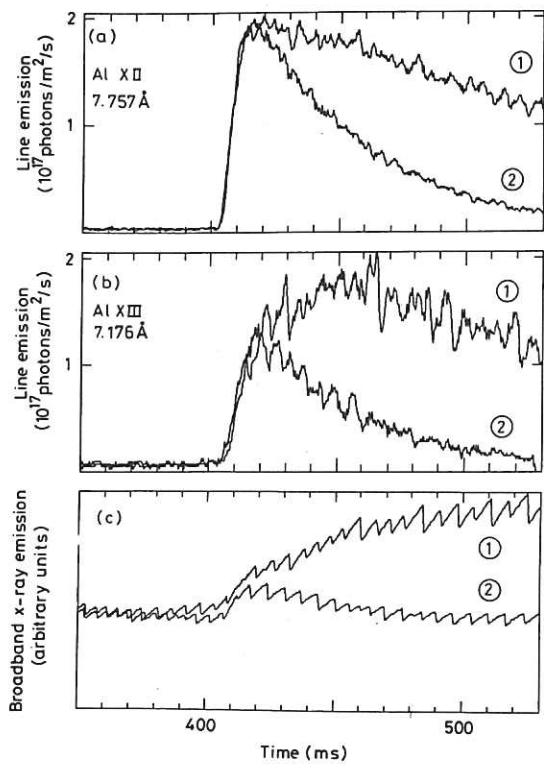


Fig.1 Spectroscopic data from aluminium injection, at 400ms, into (1) constant density discharge ($d\bar{n}_e/dt < 5 \times 10^{19} \text{m}^{-3} \text{s}^{-1}$); (2) rising density discharge ($d\bar{n}_e/dt > 1.5 \times 10^{20} \text{m}^{-3} \text{s}^{-1}$).

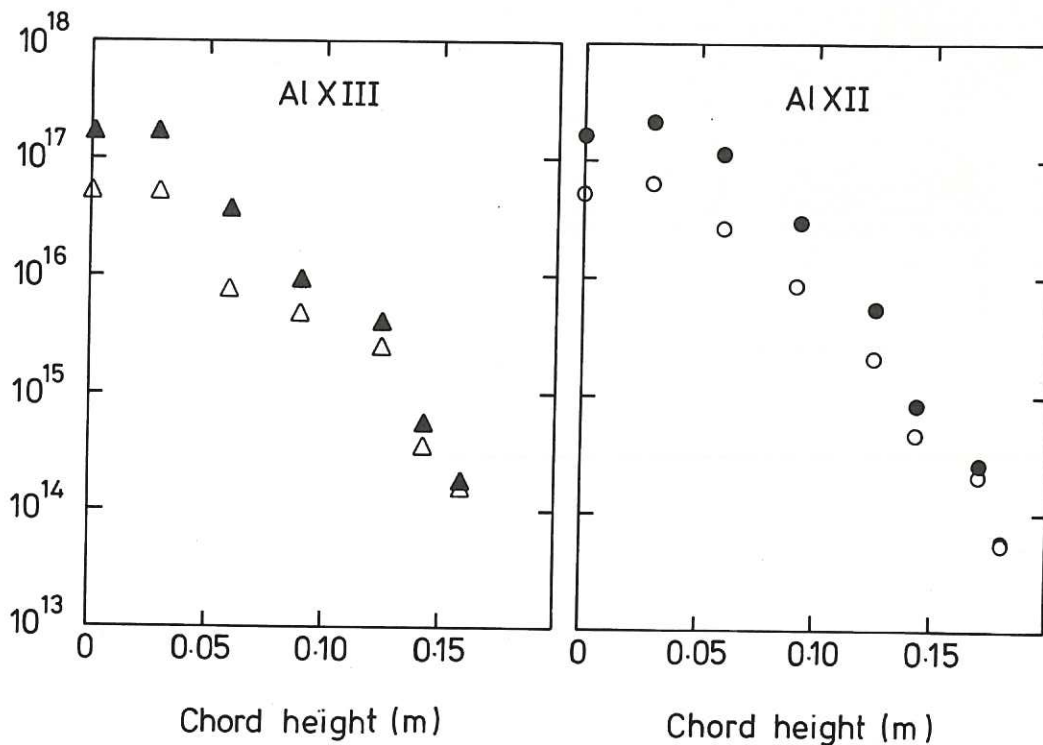


Fig.2 Spatial scans of Al XIII (7.176 Å) and Al XII (7.757 Å) line emissions as a function of chord height. Solid points: constant density, long confinement. Open points: rising density, short confinement.

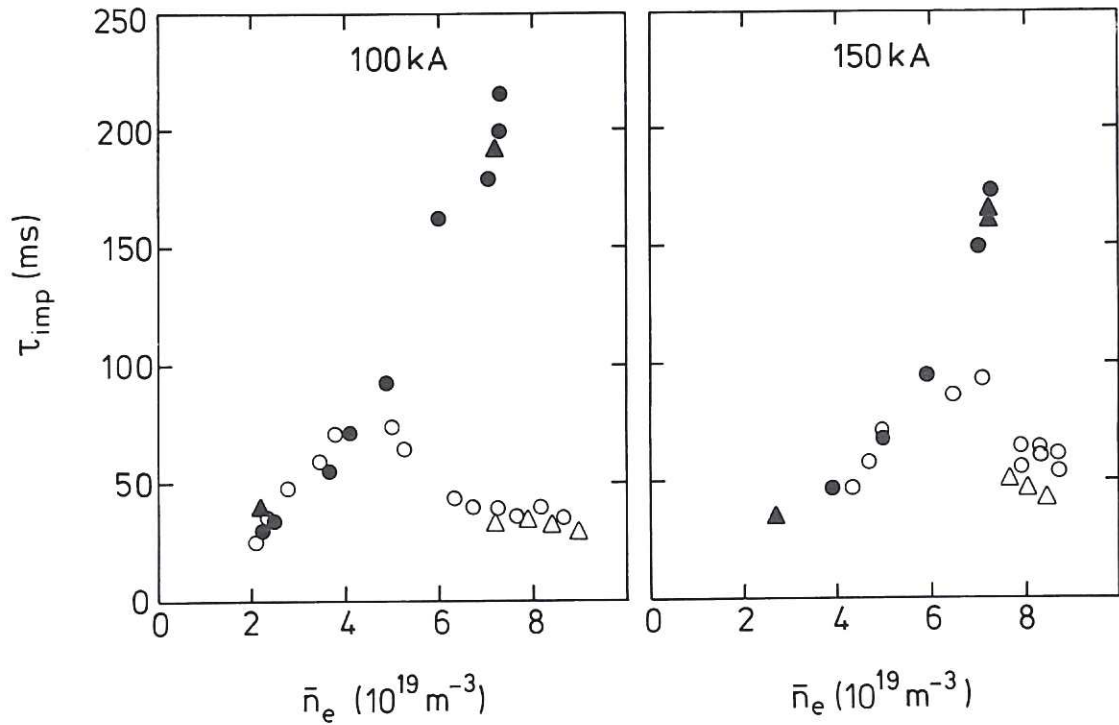


Fig.3 Variation of impurity confinement time, τ_{imp} , with mean line of sight density \bar{n}_e . Open points: rising density. Solid points: constant density. Δ , \blacktriangle Al XIII; \circ , \bullet Al XII.

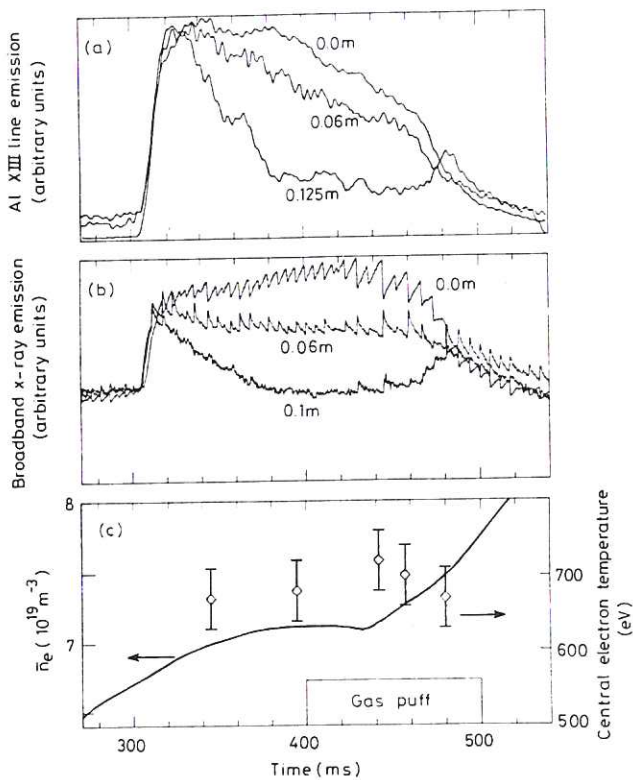


Fig.4 a,b Spatially resolved spectroscopic data for discharge with aluminium injection at 300ms. The Al XIII line emission is normalised at the peak values, the broadband X-ray emission at 300ms. c Time history of \bar{n}_e (continuous line), $T_e(0)$ (points) and gas puff.



